Int. J. Heat Mass Transfer. Vol. 27, No. 3, pp. 399–407, 1984
Printed in Great Britain

0017-9310/84 $3.00+0.00

MODELING OF THE EFFECTIVE THERMAL CONDUCTIVITY AND DIFFUSIVITY OF A PACKED BED WITH STAGNANT FLUID

EMERSON F. JAGUARIBE
Centro de Tecnologia da UFPB, Departamento de Engenharia Mecânica, Campus Universitário da UFPB, 58.000 João Pessoa, PB, Brazil

and

DONALD E. BEASLEY*
University of Michigan, Department of Mechanical Engineering and Applied Mechanics, Ann Arbor, MI 48109, U.S.A.

(*Received* 23 *December* 1982 *and in revised form* 22 *June* 1983)

Abstract—Beginning with a model of radial energy transport in a fluid saturated porous medium formed by a cubic array of cylinders with a stagnant fluid, a generalized method for determining overall effective conductivity, volumetric specific energy capacity, and effective thermal diffusivity is derived. The resulting model is not limited to any particular geometry, since it requires only the physical properties of the fluid and solid, and the void fraction as input. Comparisons demonstrate that the model agrees well with both experimental and theoretical values for the effective conductivity, while requiring no empirical or theoretical model parameters. Results for effective thermal conductivity and effective thermal diffusivity as functions of void fraction and as functions of the ratio of solid to fluid thermal conductivity are presented.

NOMENCLATURE

A	area [mm^2]
a	$\tan\lambda$
c	specific heat [kJ kg^{-1} K^{-1}]
D	parameter defined by equation (9)
D_p	particle diameter [mm]
G_m	sum of the angles which form the void region between consecutive radii
k	thermal conductivity [W m^{-1} K^{-1}]
L	bed length [mm]
q_1	heat flux [W m^{-2}]
r_{ij}	inner radius of a model void region [mm]
R	cylinder, or particle radius [mm]
R_{ij}	outer radius of a model void region
R_0	radius, defined by equation (6) (see Fig. 4) [mm]
$R11$	outer radius of the first continuous void (see Fig. 4) and defined by equations (10) and (11)
U	total thermal resistance (electrical analogy) defined by equation (18) [K W^{-1}]
U_0	thermal resistance (electrical analogy) defined by equation (13) [K W^{-1}]
U_1	thermal resistance (electrical analogy) defined by equation (14) [K W^{-1}]
W	thermal resistance (electrical analogy) defined by equation (16) [K W^{-1}]
X	thermal resistance (electrical analogy) defined by equation (17) [K W^{-1}].

Greek symbols

α	thermal diffusivity [m^2 s^{-1}]
β	angle defined by equation (5) (see Fig. 2)
γ	angle formed by the lines $\overline{01}$ and $\overline{02}$ (see Fig. 4) and defined by equation (12)
ε	bulk mean voidage
ε_1	parameter defined by equation (15)
θ	included angle of a defined void, given by expressions (4), *rd*
λ	angle, represents the void fraction in the volume $\pi/4\,(R_0^2 - R11^2)L$
ρ	density [kg m^{-3}]
ψ	function of $\tan\lambda$ [see equation (9)].

Subscripts

e	effective
f	fluid phase
i	denotes the position of the void in each section, $i = 1$ indicates the first void location from the center of the array, immediately above the axis **ox** (see Fig. 3)
j	denotes the position of the section number containing the particular void (see Fig. 3, the sections are represented by Roman numbers)
L	limiting value
m	denotes the particular radius in the composite cylinder $R_{m=1} = r_{12}$
N	indicates the outer radius of the composite medium
p	partial, referring to the shaded area in Fig. 4
s	solid

* Present address: Department of Mechanical Engineering, 318 Riggs Hall, Clemson University, Clemson, SC 29631, U.S.A.

T	total
v	void.

Superscripts

i	denotes the position of the void in each section, $i = 1$ indicates the first void location from the center of the array, immediately below the axis **oz** (see Fig. 3)
v	void
s	solid.

1. INTRODUCTION

BECAUSE of their large interphase surface area to total volume ratio, and their capability of good fluid mixing, packed beds have been used in a wide variety of processes which require an interaction between one or more fluids and one or more solids. Catalytic reactors, pebble bed heaters, evaporators, absorbers, glass furnaces, and thermal energy storage are examples of applications of packed beds.

Numerous studies have been dedicated to understanding the various physical mechanisms of flow and heat transfer in packed beds, to improve their design. Recently the storage of thermal energy in packed beds has prompted the study of transient temperature distributions in rock beds for thermal energy storage, as would be employed in solar domestic heating. During an energy collection (charging) period, a temperature distribution, or thermocline, will be established in the packed bed; if there is not an immediate demand for this stored energy, the thermocline will decay, with the associated loss in available energy. For downward flow during charging, an inherently unstable temperature distribution is established in the upper regions of the bed, since the outlet temperature from the collector decreases after reaching a maximum near solar noon. Therefore, both natural convection and pure diffusion may contribute to the thermocline degradation in various regions of the bed. As an aid to understanding the importance of this natural convection, in addition to the previously mentioned applications, a reasonable value for the effective thermal conductivity, and effective thermal diffusivity in a stagnant packed bed is needed. However, as Pai and Raghavan [1] report, the problem of determining the thermal conductivity of a heterogeneous system has defied analytical solution for a considerable time.

The general problem of determining the overall effective thermal conductivity of a porous medium may be approached by one of two basic ways:

(1) The overall value is taken as an appropriate average of the separate phase contributions.

(2) Transport among individual particles in a regular array is extended to the entire medium.

In a medium composed of a solid phase and a gas phase, the averages over the separate phases assume that conduction through the solid acts over a volume $1-\varepsilon$ and the conduction through the gas in the void spaces over a fluid volume ε. This approach has been used not only to determine the effective thermal conductivity of a porous system, but also the electrical conductivity, magnetic permeability, coefficient of diffusion, etc. of heterogeneous media (cf. Wyllie [2], Dul'nev and Norikov [3, 4], Beveridge and Haughey [5], etc.). Often this method reduces to an analogous electrical network. For random packings the effective parameters are determined using unit cell elements of regular packings, again with appropriate averages. The simplest models use the arithmetic mean of the contributions from each phase; others use harmonic or geometric means. However, the more realistic models make use of experimentally determined statistical parameters, even for regular packings (cf. Tsao [6] and Cheng and Vachon [7]).

The method of extending transport among a few particles to the entire packing is exemplified by the works of Kunii and Smith [8] and Yagi and Kunii [9]. Parameters related to the angle bounding the heat flow area for one contact point, the number of contact points, etc. are required in the work by Kunii and Smith, and the total area of perfect contact surfaces, effective thickness of the fluid film in the void space relative to the thermal conduction effects, etc. for the model by Yagi and Kunii. Thus, these models require empirical or theoretical parameters other than the physical properties of the bed and packing materials; still other parameters are needed to account for radiation effects, if the bed is operated at high temperatures.

Krupiczka [10] presents an interesting comprehensive analytical study of the thermal conductivity of packed beds, which expresses the thermal conductivity in terms of the properties of the bed. Assuming models composed of both cylinders and spheres, solutions are obtained by non-orthogonal series methods. Since these results are difficult to utilize effectively, approximations with simpler functions are derived. Existing experimental data is then used to develop a correlation in terms of the bulk mean voidage and k_s/k_f. The resulting expression is independent of the particle diameter and length of the bed. Thus, Krupiczka's model results in identical values of thermal conductivity for beds with equal void fraction and solid and fluid, regardless of the particle diameter or geometrical dimensions for the bed.

The present work was directed toward finding the effective thermal conductivity and effective thermal diffusivity of a stagnant packed bed, at a low mean temperature where radiation effects are small, using only the void fraction, thermal properties of the solid and fluid, and the solid and fluid densities. To accomplish this, a specific geometry is assumed for the porous media, from which a generalized arrangement of solid and fluid regions is specified, the relative volumes of which are governed by the bulk mean void fraction, ε. As such the final model is independent of the specific geometry of the actual packing but rather is a generalized model for diffusion in a porous media.

2. PROPOSED MODEL

It is desired to analyze the transport of thermal energy in a fluid saturated porous medium composed of cylinders, arranged as shown in Fig. 1, with the central cylinder as the source of the energy. From symmetry, only the shaded region, with an included angle of $\pi/4$ must be considered in the analysis. Conduction through the two phases, solid and fluid, is assumed to be the only mechanism for energy transport, implying that the fluid phase is stagnant and radiation effects may be neglected. Hereafter the fluid phase will be referred to as 'void' regions. Conduction through the contact points between discrete solid particles is included in the model as regions of continuity in the solid phase (see Fig. 3).

2.1. *General considerations*

In this approach, the existing arrangement of solid and void regions will be replaced by an equivalent arrangement of solid and void, whose geometry is more amenable to calculating the overall effective conductivity. The original voids are each replaced by a void placed within two concentric cylinders of radii r_{ij} and R_{ij}, and within the angle θ_j^i (see Figs. 2 and 3). The model geometry is thus divided into sections, with the index j denoting the section number containing the particular void. A section is defined as the region bounded by two planes perpendicular to the axis **ox**, each containing the axis of one of the two neighboring cylinders, and the axes **ox** and **oz**. (For example, the first section, Fig. 3, is the triangular area OA′A.) The index i denotes the position of the void in each section; the subscript i indicates the first void location from the center of the array, immediately above the axis **ox**. With these definitions, r_{ij} may be determined from the expression

$$r_{ij} = [(2j-1)^2+4(i-1)^2]^{1/2}R. \tag{1}$$

In the proposed arrangement of solid and fluid, the volume of the model voids must be individually equal to the volume of the voids they replace. To accomplish this, R_{ij} is given by

$$R_{ij} = \left[\frac{8\varepsilon}{\theta_j^{j-i-1}}R^2+r_{ij}^2\right]^{1/2}, \tag{2}$$

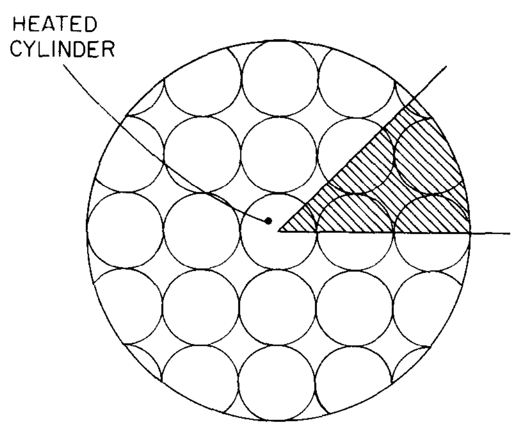

FIG. 1. Diagram of the arrangement of cylinders forming the porous medium.

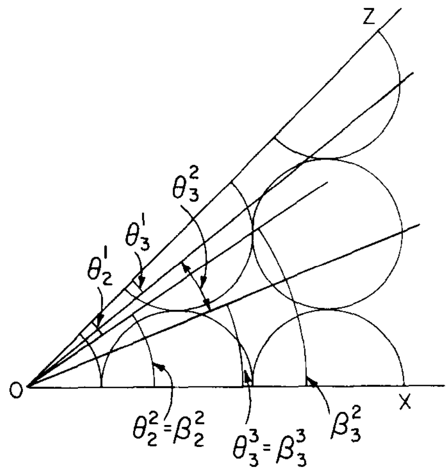

FIG. 2. Description of the angles θ_j^i and β_j^i.

when $i \neq j$, and by

$$R_{ij} = \left[\frac{4\varepsilon}{\theta_j^{j-i-1}}R^2+r_{ij}^2\right]^{1/2}, \tag{3}$$

when $i = j$. The included angle for each new void is given by

$$\begin{aligned} \theta_j^j &= \beta_j^j, \\ \theta_j^{j-i} &= \beta_j^{j-i}-\beta_j^j, \\ \theta_j^1 &= \frac{\pi}{4}-\beta_j^2, \end{aligned} \tag{4}$$

if $j \geq 2$, where

$$\beta_j^i = \tan^{-1}\left[\frac{2(1+j-i)}{2j-1}\right]. \tag{5}$$

The radii r_{ij} and R_{ij}, defined above, are used to characterize the model voids, beginning with section two of the model geometry. The void associated with the central cylinder will be considered as a special case.

Since the central cylinder is contacted by other cylinders only in line contacts, it is appropriate to consider the central cylinder as being surrounded by void region of radius $R11$. R_0 is defined by

$$R_0 = \left(\frac{16}{\pi}\right)^{1/2}R. \tag{6}$$

With R_0 so defined, it is necessary to specify $R11$, such that the volume bounded by R and $R11$ is void and between $R11$ and R_0 both solid and void regions exist, with a common interface along the line which makes an angle λ with **ox**. Then $4\lambda/\pi$ represents the void fraction in the volume $(\pi/4)(R_0^2-R11^2)L$.

The total void fraction in the volume bounded by R_0 and $\theta = \pi/4$ is given by

$$2\varepsilon R^2 = \frac{\pi}{8}(R11^2-R^2)+\frac{\lambda}{2}(R_0^2-R11^2). \tag{7}$$

Solving this equation for $R11$ yields

$$R11 = \left[\frac{(16\varepsilon+\pi)R^2-\lambda R_0^2}{\pi-4\lambda}\right]^{1/2}. \tag{8}$$

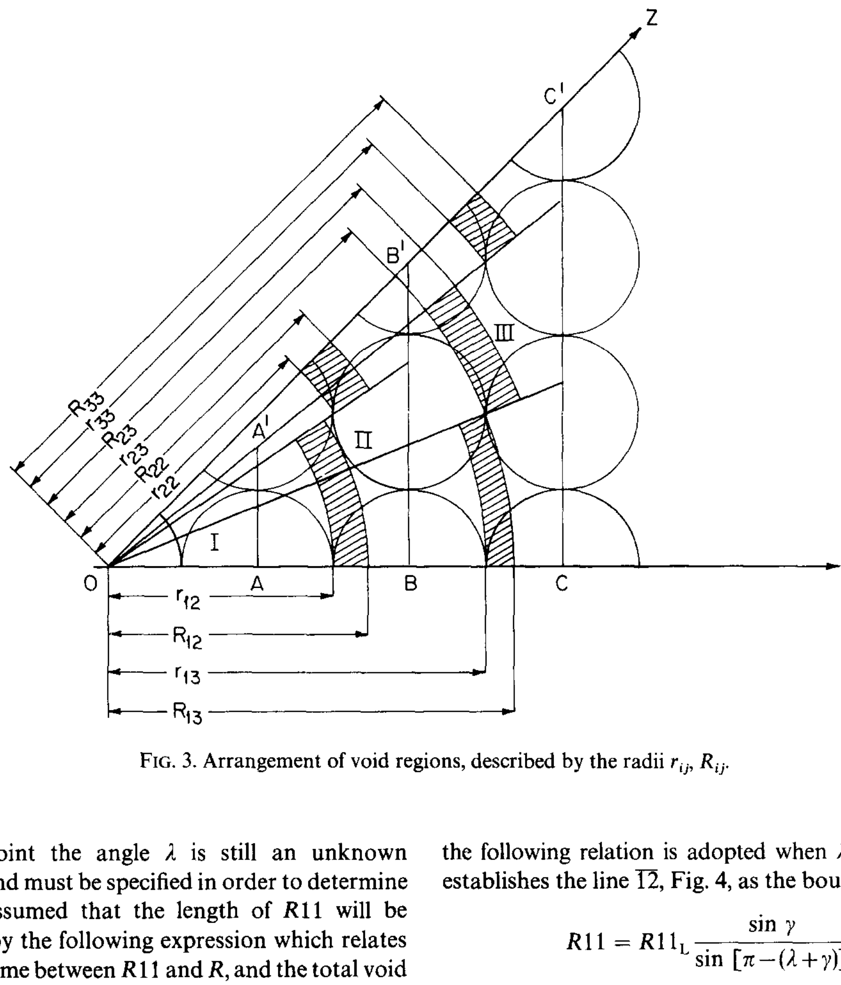

FIG. 3. Arrangement of void regions, described by the radii r_{ij}, R_{ij}.

At this point the angle λ is still an unknown parameter, and must be specified in order to determine $R11$. It is assumed that the length of $R11$ will be determined by the following expression which relates the solid volume between $R11$ and R, and the total void volume bounded by R and R_0. The ratio of these volumes is D, and for this work is assumed to be 0.05, yielding

$$D = \frac{A_p^s}{A_T^v} = \left[0.5(\sin^{-1}\psi) - \psi + 0.5\frac{\lambda R11^2}{R^2}\right]\frac{1}{2\varepsilon} = 0.05, \quad (9)$$

where

$$\psi = \frac{a[2-(1-3a^2)^{1/2}]}{1+a^2},$$

where $a = \tan\lambda\,(\lambda \leqslant \pi/8)$, A_p^s is the shaded area in Fig. 4 and A_T^v is the total void area in the section. The value of D was selected by first determining from the geometry that the ratio was very small, of the order of 0.05 or less. A range of values were employed, to determine the sensitivity of the solution to changes in D. For $D \leqslant 0.02$ problems existed in the solution to equation (10), from which λ is determined. Computing times increase significantly for $D < 0.05$; results obtained for values of D from 0.03 to 0.05 show no significant difference. Thus $D = 0.05$ is used for this study

$$\lambda\left(\frac{R11}{R}\right)^2 = 0.2\varepsilon - \sin^{-1}\psi + 2\psi. \quad (10)$$

Since for $\lambda > \pi/8$ the values of $R11$ increase faster than for values of $\lambda < \pi/8$, and when $\lambda = \pi/4$, $R11 = R_0$, the following relation is adopted when $\lambda > \pi/8$, which establishes the line $\overline{12}$, Fig. 4, as the boundary for $R11$

$$R11 = R11_L \frac{\sin\gamma}{\sin[\pi-(\lambda+\gamma)]}. \quad (11)$$

$R11_L$ is obtained from the equation (10) for $\lambda = \pi/8$ and

$$\gamma = \frac{7\pi}{8} - \tan^{-1}\frac{\overline{01}\sin\pi/8}{R_0 - \overline{01}\cos\pi/8}. \quad (12)$$

It is clear that equations (10) and (11) are transcendental, and must be solved by iteration.

With the geometry so defined, the diffusion of thermal energy may now be analyzed.

2.2 *Analysis of energy transport*

Utilizing the proposed geometric model of a generalized porous medium, the effective conductivity of the stagnant fluid case for the overall arrangement may be determined. If we assume that a specified heat flux, q_1, is flowing from the central cylinder, of radius R, limited by an angular range $0 \leqslant \theta \leqslant \pi/4$, the proposed geometry may be treated as a composite conduction medium, with defined solid and fluid regions. Using an electrical analogy, the system is represented by four resistances in series

$$U_0 = \frac{\ln(R11/R)}{k_s(\pi/4)L}, \quad (13)$$

$$U_1 = \frac{\ln(R_0/R11)}{[(1-\varepsilon_1)k_s + \varepsilon_1 k_f](\pi/4)L}, \quad (14)$$

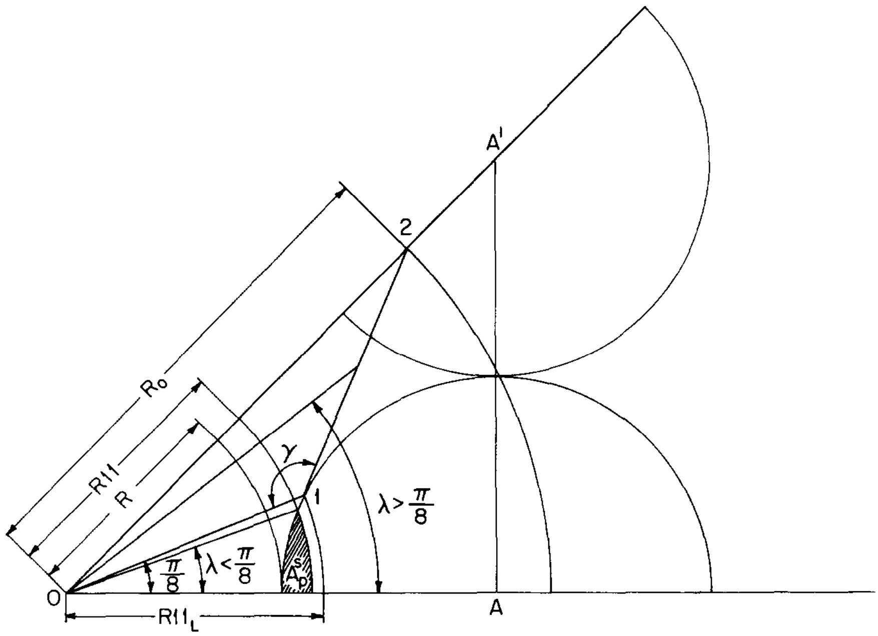

FIG. 4. Section I showing area A_p^s, radius $R11$, $R11_L$, R_0 lines $\overline{01}$ and $\overline{12}$, and angles λ and γ.

where

$$\varepsilon_1 = \frac{4\lambda}{\pi}, \tag{15}$$

$$W = \frac{\ln (R_{12}/R_0)}{k_s(\pi/4)L}, \tag{16}$$

and

$$X = \sum_{m=1}^{N-1} \frac{\ln (R_{m+1}/R_m)}{[k_s(\pi/4 - G_m) + k_f G_m]L}. \tag{17}$$

G_m represents the sum of the angles that form the void region between R_m and R_{m+1}, where R_{m+1} and R_m are two consecutive radii of the composite cylindrical solid/void model, beginning with r_{12} and ending with the external radius of the composite conduction medium. This method of defining X, which determines the locations of the voids in the model geometry, contributes to the extended validity of the model for cases where the void (fluid phase) is randomly distributed in a given system. Since equations (2) and (3) are written in terms of a bulk mean voidage, ε, the structural development of the model is not a limiting factor, and the model is easily extended to other geometric arrangements, with their associated variations in ε. Therefore, although the model is developed for a particular geometry, the result is applicable to other geometries by allowing ε to vary. It is also apparent that the model is equally valid for any two distinct materials, fluid and solid, or just solids.

The overall resistance to the flow of energy, in analogy to an electrical circuit, is given by

$$U = U_0 + U_1 + W + X, \tag{18}$$

and the overall effective thermal conductivity

$$k_e = \frac{\ln (R_N/R)}{(\pi/4)UL}, \tag{19}$$

where $R_N = L$.

Also, the thermal diffusivity of a medium controls the diffusion of energy in a purely conductive mode. As such, the property of interest for the study of thermocline degradation in a packed bed for thermal energy storage is the effective thermal diffusivity

$$\alpha_e = \frac{k_e}{(1-\varepsilon)\rho_s c_s + \varepsilon \rho_f c_f}. \tag{20}$$

The denominator of the function is linear in ε, while k_e is a complex function of several parameters. This implies that for a given packed bed, the effective thermal diffusivity depends strongly on the void fraction and the fluid and solid properties. To validate the model, it must be tested for a number of packings, including variations in void and packing particle shape and size.

3. RESULTS AND DISCUSSION

The proposed method of solution was programmed for an IBM Personal Computer, with the required input parameters of length of packing traversed by the energy, L, the average spherical particle diameter, D_p, the bulk mean voidage, ε, and the thermal conductivities of the solid and fluid phases, k_s and k_f, respectively. For purposes of comparison, calculations of effective conductivities were made for the experimental cases reported in the summary by Ofuchi and Kunii [11] and one measured value by Beveridge and Haughey [5]. The results of these calculations

Table 1

Case	D_p (mm)	ε	k_s/k_f	Fluid	Solid	L (mm)	Exp.	k_e/k_f Ofuchi and Kunii [11]	k_e/k_f Present authors
1	12.1	0.376	0.90	Water	Glass spheres	50	0.87	0.94	0.94
2	8.7	0.369	0.90	Water	Glass spheres	50	0.90	0.94	0.94
3	6.38	0.337	0.90	Water	Glass spheres	50	0.94	0.94	0.94
4	3.69	0.369	0.90	Water	Glass spheres	50	0.96	0.94	0.94
5	3.69	0.34	0.90	Water	Glass spheres	50	0.90	0.94	0.94
6	2.66	0.34	0.90	Water	Glass spheres	50	0.90	0.94	0.94
7	3.69	0.369	3.7	He	Glass spheres	50	2.46	2.40	2.35
8	6.38	0.358	3.7	He	Glass spheres	50	2.46	2.38	2.40
9	8.70	0.369	3.7	He	Glass spheres	50	2.49	2.43	2.32
10	3.69	0.369	31	CO_2	Glass spheres	50	8.61	8.89	9.12
11	6.38	0.337	31	CO_2	Glass spheres	50	8.24	9.25	9.40
12	8.70	0.369	31	CO_2	Glass spheres	50	9.40	9.07	7.98
13	1.15	0.340	21	Air	Glass spheres	50	6.38	6.40	6.23
14	3.69	0.369	21	Air	Glass spheres	50	6.71	7.03	7.49
15	6.38	0.337	21	Air	Glass spheres	50	7.13	7.38	7.71
16	6.38	0.358	21	Air	Glass spheres	50	7.49	6.97	7.32
17	8.70	0.369	21	Air	Glass spheres	50	7.78	7.26	6.74
18	3.09	0.390	1650	Air	Steel balls	50	10.1	16.6	16.61
19	3.09	0.342	1650	Air	Steel balls	50	15.0	21.5	22.29
20	10.9	0.403	1650	Air	Steel balls	50	18.6	15.5	11.20
21	3.09	0.413	1650	Air	Steel balls	50	11.2	13.9	15.30
22	6.32	0.396	1650	Air	Steel balls	50	10.4	17.2	14.32
23	6.32	0.352	1650	Air	Steel balls	50	29.0	20.9	16.94
24	6.32	0.352	2370	CO_2	Steel balls	50	42.7	22.5	17.03
25	3.09	0.342	2370	CO_2	Steel balls	50	22.1	22.9	20.17
26	3.09	0.39	294	He	Steel balls	50	6.65	12.1	14.77
27	10.9	0.403	70	Water	Steel balls	50	6.28	8.54	8.80
28	8.18	0.475	59	Air	Rashig rings	50	7.47	6.69	6.99
29	5.12	0.572	59	Air	Rashig rings	50	7.39	5.56	5.60
30	5.12	0.603	59	Air	Rashig rings	50	6.64	5.32	4.79

Table 2

Case	D_p (mm)	ε	k_s/k_f	Fluid	Solid	L (mm)	Exp.	k_e/k_f Ofuchi and Kunii [11]	k_e/k_f Present authors
31	8.18	0.475	87	CO_2	Rashig rings	50	10.0	8.51	7.53
32	5.12	0.603	87	CO_2	Rashig rings	50	7.95	6.38	5.15
33	5.12	0.572	10.4	He	Rashig rings	50	2.31	2.66	3.06
34	8.18	0.475	2.53	Water	Rashig rings	50	1.11	1.53	1.67
35	5.12	0.603	2.53	Water	Rashig rings	50	0.98	1.39	1.46
36	7.31	0.366	34	Air	Cement clinkers	50	8.92	9.10	8.75
37	7.31	0.370	34	Air	Cement clinkers	50	7.40	8.10	8.65
38	7.31	0.370	50	CO_2	Cement clinkers	50	9.02	10.0	9.98
39	7.31	0.366	5.9	He	Cement clinkers	50	3.34	2.70	3.23
40	7.31	0.370	1.44	Water	Cement clinkers	50	1.24	1.13	1.25
41	2.45	0.359	7.4	He	River sand	50	3.19	3.5	3.62
42	2.45	0.359	1.78	Water	River sand	50	1.77	1.4	1.41
43	2.45	0.359	42	Air	River sand	50	8.20	8.50	10.49
44	4.75	0.384	12.6	Air	Nickel catalyst pellets	50	5.46	4.9	5.12
45	4.75	0.384	18.5	CO_2	Nickel catalyst pellets	50	6.73	6.17	6.46
46	4.75	0.384	2.22	He	Nickel catalyst pellets	50	1.45	1.69	1.62
47	4.75	0.384	1.82	H_2	Nickel catalyst pellets	50	1.20	1.48	1.43
							Masamune and Smith [12]	Beveridge and Haughey [5]	
48	0.47	0.38	38.53	Air	Glass sphere	12.7	6.62	6.40	7.06

appear in Tables 1 and 2. The mean bed temperature in the data of Ofuchi and Kunii was $\sim 50°C$, so that radiative effects are relatively small. In general, the proposed stagnant fluid, conductive model is in good agreement with both the experimentally determined values and the predictions by Ofuchi and Kunii. However, there are specific cases for both models where the experimentally determined values are quite different than the predicted values (i.e. Cases 18, 22, 23, 24, 26, 27, and 31). Error bounds for the experimental data could not be determined. However, the present authors could find no reasonable pattern of discrepancy to indicate a particular physical explanation as the primary reason for the differences. In any case, for physical systems as complex as these, the predictions are quite reasonable, and follow the gross behavior of the overall effective conductivity quite well, both for the present model and that of Ofuchi and Kunii. It should be noted that the more complex model of Ofuchi and Kunii shows significant deviation from the measured values in many of the same cases as the present authors' model. Also the present model appears valid for packings of irregular particles, producing reasonable values for the effective thermal conductivity. The model of Krupiczka [10] was compared with the values of k_e found in Tables 1 and 2. For $k_s/k_f \geqslant 1650$ this model predicted k_e values consistently higher than the experimental data and the model of Ofuchi and Kunii, and the present model. For $k_s/k_f \leqslant 294$ the trend is reversed.

Figure 5 shows plots of α_e/α_f and k_e/k_f for the practical range of values of ε for a packed bed. A solid line is used to characterize the range of ε where experimental data are available. In these units, k_e/k_f and α_e/α_f are monotonic functions of ε, with a limiting value for both curves as ε approaches 0.8. From $\varepsilon = 0.7$ to 0.8 the value of k_e/k_f continues to decrease while α_e/α_f represented by a dashed line, exhibits a change in slope. Further experimental study is required to determine the nature of the physical phenomena in this range of void fraction. Figure 6 demonstrates the rapid increase of k_e/k_f for $2 < \ln(k_e/k_f) < 5$ with limiting values quickly reached outside this range.

4. CONCLUSIONS

Beginning with a cubic arrangement of cylinders, a general arrangement of solid and void regions has been developed which allows for calculation of the overall effective conductivity and the overall effective thermal diffusivity of a packed bed. The model requires only the void fraction of the packing and the solid and fluid properties. Comparisons with experimental data and predictions for a range of void fraction, fluid and solid properties, and packing particle shape and size distributions show good agreement. This model may then be used to approximate the effective thermal conductivity and effective thermal diffusivity of a packed bed with a stagnant fluid phase. Also, knowing the effective conductivity of a stagnant bed will allow the effect of natural convective motion in the fluid to be assessed.

The model might be improved by starting from a three-dimensional spherical geometry, rather than a cubic packing of cylinders. An additional improvement may result from the introduction of radiative transfer in the void spaces, in cases of high temperature operation.

The range of void fraction studied experimentally is

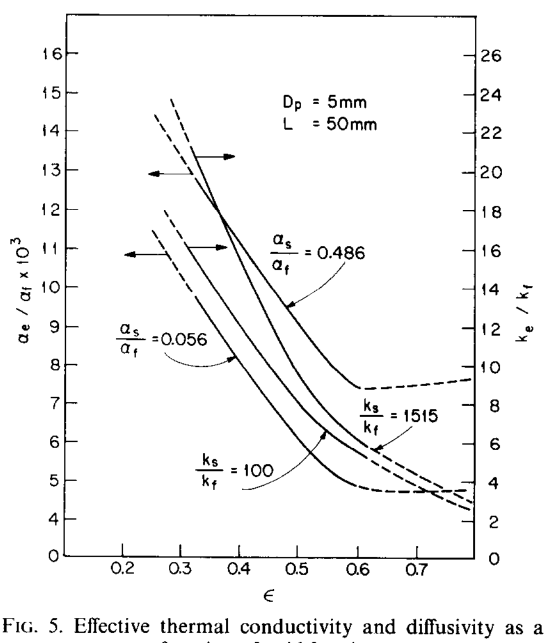

FIG. 5. Effective thermal conductivity and diffusivity as a function of void fraction.

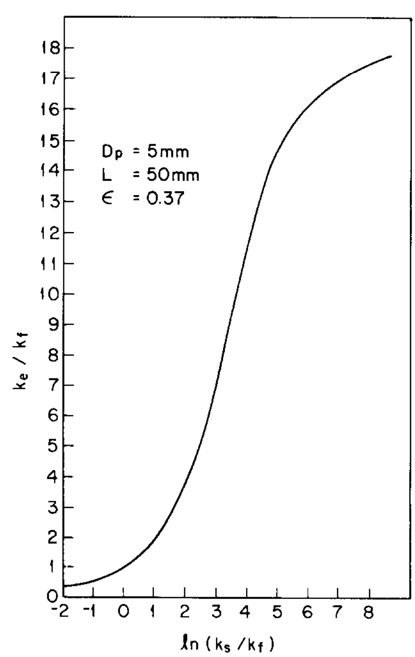

FIG. 6. Effective thermal conductivity as a function of $\ln(k_s/k_f)$.

small, and further comparisons would be useful, especially in the range of void below 0.3. Values of ε down to 0.0931 can be achieved with regular packings of cylinders, so that additional comparisons are possible.

Acknowledgements—The first author was supported by Conselho Nacional de Desenvolvimento Cientifico e Tecnológico, CNPq, Brazil, while a Visiting Professor in the Solar Energy Laboratory, Department of Mechanical Engineering and Applied Mechanics, University of Michigan. The authors would like to express their thanks to Dr John A. Clark for his support and guidance, and to the Department of Mechanical Engineering and Applied Mechanics for use of the facilities.

REFERENCES

1. K. Pai and V. R. Raghavan, A thermal conductivity model for two phase media, *Lett. Heat Mass Transfer* **9**, 21–27 (1982).
2. M. R. J. Wyllie, An experimental investigation of the S.P. and resistivity phenomena in dirty sands, *J. Petrol. Technol. Trans. AIME* **199**, 44–47 (1954).
3. G. N. Dul'nev and V. V. Norikov, Conductivity determination for a filled heterogeneous system, *J. Engng Phys.* **37**, 657–661 (1979).
4. G. N. Dul'nev and V. V. Norikov, Conductivity of nonuniform systems, *J. Engng Phys.* **36**, 901–909 (1979).
5. G. S. G. Beveridge and D. P. Haughey, Axial heat transfer in packed beds, stagnant beds between 20 and 750°C, *Int. J. Heat Mass Transfer* **14**, 1093–1113 (1971).
6. G. T. Tsao, Thermal conductivity of two phase materials, *Ind. Engng Chem.* **53**, 395–399 (1961).
7. S. C. Cheng and R. I. Vachon, Prediction of the thermal conductivity of two and three phase solid heterogeneous mixtures, *Int. J. Heat Mass Transfer* **12**, 249–264 (1969).
8. D. Kunii and J. M. Smith, Heat transfer characteristics of porous rocks, *A.I.Ch.E. Jl* **6**, 71–77 (1960).
9. S. Yagi and D. Kunii, Studies on effective thermal conductivities in packed beds, *A.I.Ch.E. Jl* **3**, 373–381 (1957).
10. R. Krupiczka, Analysis of thermal conductivity in granular materials, *Int. Chem. Engng* **7**, 122–144 (1967).
11. K. Ofuchi and D. Kunii, Heat transfer characteristics of packed beds with stagnant fluids, *Int. J. Heat Mass Transfer* **8**, 749–757 (1965).
12. S. Masamune and J. M. Smith, Thermal conductivity of beds of spherical particles, *Ind. Engng Chem. Fundam.* **2**, 136–143 (1963).

MODELISATION DE LA CONDUCTIVITE THERMIQUE ET DE LA DIFFUSIVITE EFFECTIVES D'UN LIT FIXE AVEC UN FLUIDE STAGNANT

Résumé—A partir d'un modèle de transport radial d'énergie dans un milieu poreux saturé de fluide et formé d'un arrangement cubique de cylindres avec un fluide stagnant, on propose une méthode générale pour déterminer la conductivité globale effective, la capacité thermique volumique et la diffusivité thermique effective. Le modèle n'est pas limité à une géométrie particulière puisqu'il requiert seulement la connaissance des propriétés physiques du fluide et du solide et de la fraction de vide. Des comparaisons montrent que le modèle s'accordent bien avec les valeurs expérimentales et théoriques pour la conductivité effective. On présente des résultats pour la fraction de vide et du rapport des conductivités du solide et du fluide.

MODELLBILDUNG DER EFFEKTIVEN WÄRMELEITFÄHIGKEIT UND TEMPERATURLEITFÄHIGKEIT EINES FESTBETTES MIT RUHENDEM FLUID

Zusammenfassung—Zunächst wird ein Modell entwickelt für den radialen Wärmetransport in einem mit Fluid gesättigten porösen Medium, das aus einer kubischen Anordnung von Zylindern mit ruhendem Fluid besteht. Daraus ergibt sich eine verallgemeinerte Methode, um die effektive Wärmeleitfähigkeit, die volumetrische spezifische Wärmekapazität und die effektive Temperaturleitfähigkeit zu ermitteln. Das entstehende Modell ist nicht auf eine besondere Geometrie beschränkt, da es nur die physikalischen Stoffwerte der Flüssigkeit und des Feststoffs und die Porosität als Eingabegrößen benötigt. Vergleiche zeigen, daß das Modell gut mit experimentellen und theoretischen Werten für die effektive Leitfähigkeit übereinstimmt, ohne empirische oder theoretische Modellparameter zu benötigen. Ergebnisse für die effektive Wärmeleitfähigkeit und die effektive Temperaturleitfähigkeit werden als Funktionen der Porosität und des Verhältnisses aus Feststoff- und Fluidwärmeleitfähigkeit dargestellt.

МОДЕЛИРОВАНИЕ ЭФФЕКТИВНОЙ ТЕПЛОПРОВОДНОСТИ И ТЕМПЕРАТУРОПРОВОДНОСТИ ПЛОТНОГО СЛОЯ С НЕПОДВИЖНОЙ ЖИДКОСТЬЮ

Аннотация—Исходя из модели радиального энергопереноса в насыщенной жидкостью пористой среде, образованной кубической решеткой из цилиндров, заполненной неподвижной жидкостью, предложен обобщенный метод определения средней эффективной теплопроводности, объемной удельной теплоемкости и эффективного коэффициента температуропроводности. Предложенная модель не ограничена какой-либо геометрией, так как в нее заложены только физические свойства жидкости, твердого тела и коэффициента пористости. Сравнения показывают, что модель хорошо согласуется как с экспериментальными, так и с теоретическими данными для эффективной теплопроводности, не требуя введения ни эмпирических, ни теоретических параметров. Представлены результаты для эффективных теплопроводности и температуропроводности как функций коэффициента пористости и отношения теплопроводности твердого тела к теплопроводности жидкости.